OXFORD

Social Cognitive and Affective Neuroscience, 2017, 1284–1295

doi: 10.1093/scan/nsx050
Advance Access Publication Date: 7 April 2017
Original article

Social anxiety disorder exhibit impaired networks involved in self and theory of mind processing

Qian Cui,[1,2] Eric J. Vanman,[3] Zhiliang Long,[2] Yajing Pang,[2] Yuyan Chen,[2] Yifeng Wang,[2] Xujun Duan,[2] Heng Chen,[2] Qiyong Gong,[4] Wei Zhang,[5] and Huafu Chen[2]

[1]School of Political Science and Public Administration, University of Electronic Science and Technology of China, Chengdu, 611731, China, [2]Key Laboratory for Neuroinformation of Ministry of Education, Center for Information in BioMedicine, School of Life Science and Technology, University of Electronic Science and Technology of China, Chengdu, 611731, China, [3]School of Psychology, University of Queensland, St. Lucia, QLD, Australia, [4]Huaxi MR Research Center, Department of Radiology, West China Hospital of Sichuan University, West China School of Medicine, Chengdu, 610041, China, and [5]Mental Health Center, West China Hospital of Sichuan University, Chengdu, 610041, China

Correspondence should be addressed to Qian Cui, School of Political Science and Public Administration, University of Electronic Science and Technology of China, Chengdu, 611731, China. E-mail: qiancui26@gmail.com; Huafu Chen, Key Laboratory for Neuroinformation of Ministry of Education, Center for Information in BioMedicine, School of Life Science and Technology, University of Electronic Science and Technology of China, Chengdu, 611731, China. E-mail: chenhf@uestc.edu.cn

Abstract

Most previous studies regarding social anxiety disorder (SAD) have focused on the role of emotional dysfunction, while impairments in self- and theory of mind (ToM)-processing have relatively been neglected. This study utilised functional connectivity density (FCD), resting-state functional connectivity (RSFC) and discriminant analyses to investigate impairments in self- and ToM-related networks in patients with SAD. Patients with SAD exhibited decreased long-range FCD in the right rostral anterior cingulate cortex (rACC) and decreased short-range FCD in the right superior temporal gyrus (STG)—key nodes involved in self- and ToM-processing, respectively. Decreased RSFC of the right rACC and STG with widespread frontal, temporal, posteromedial, sensorimotor, and somatosensory, regions was also observed in patients with SAD. Altered RSFC between the right rACC and bilateral superior frontal gyrus, between the right rACC and right middle frontal gyrus, and within the right STG itself provided the greatest contribution to individual diagnoses of SAD, with an accuracy of 84.5%. These results suggest that a lack of cognitive inhibition on emotional self-referential processing as well as impairments in social information integration may play critical roles in the pathomechanism of SAD and highlight the importance of recognising such features in the diagnosis and treatment of SAD.

Key words: social anxiety disorder; self-processing; theory-of-mind; functional connectivity density; discriminant analysis

Received: 16 May 2016; **Revised:** 9 February 2017; **Accepted:** 2 April 2017

Introduction

Social anxiety disorder (SAD) is characterised by fear and avoidance of social situations, and feelings of humiliation and embarrassment due to potential scrutiny and negative evaluation by others (Stein and Stein, 2008; American Psychiatric Association, 2013). Although many studies have emphasised the role of emotional dysfunction in the pathophysiology of SAD (Phan *et al.*, 2006; Etkin and Wager, 2007), the contribution of impairments in self- and theory-of-mind (ToM)-processing remain relatively unexamined (Moscovitch, 2009; Morrison and Heimberg, 2013).

Alterations in self-processing have been associated with certain behavioural aspects of SAD, including maladaptive self-focused attention, negative self-referential processing and distorted negative self-beliefs (Goldin *et al.*, 2013a, b; Morrison and Heimberg, 2013). SAD has consistently been associated with dysfunctional activation in the ventromedial prefrontal cortex/rostral anterior cingulate cortex (rACC) (Kilts *et al.*, 2006; Heitmann *et al.*, 2014), dorsomedial prefrontal cortex and posteromedial regions (Goldin *et al.*, 2012) during self-processing. Furthermore, altered functional connectivity within and across the "default mode network", which has also been implicated in self-processing has been observed in patients with SAD (Liao *et al.*, 2010; Liu *et al.*, 2013, 2014).

Given that excessive fear of negative evaluation by others is the primary symptom of SAD (Stein and Stein, 2008; American Psychiatric Association, 2013), impairments in the ability to detect and understand the mental states of others (i.e. ToM) likely influence the capacity for patients with SAD to interpret social situations (Frith and Frith, 2005). Indeed, preliminary behavioural studies have demonstrated that patients with SAD attribute beliefs and intentions to others in contextually inappropriate ways (Hezel and McNally, 2014; Buhlmann *et al.*, 2015). In addition, recent neuroimaging studies have demonstrated structural and functional alterations in regions involved in ToM-processing, including the superior temporal gyrus (STG) (Goldin *et al.*, 2014), inferior temporal gyrus and temporal pole (TPO) (Tillfors *et al.*, 2002; Talati *et al.*, 2013; Klumpp *et al.*, 2014), in patients with SAD when compared with healthy control (HC) participants.

Although some behavioural evidence has been published regarding the role of impaired self- and ToM-processing in SAD, research regarding the neural mechanisms underlying such impairments is limited. Existing studies have focused mainly on single-region dysfunction (Tillfors *et al.*, 2002; Goldin *et al.*, 2009a, 2013a, b), while whether and how regions associated with self- and ToM-processing exhibit impaired functional connectivity with various brain regions in SAD remains to be investigated. Therefore, we first applied functional connectivity density (FCD) analysis (Tomasi and Volkow, 2010)—a voxel-wise, data-driven, graph theory approach—for the general detection of regions exhibiting altered connectivity density with other regions throughout the brain. Unlike traditional voxel-wise functional connectivity analysis, which simply describes functional connectivity of the brain, FCD can identify highly connected regions known as functional hubs (Tomasi and Volkow, 2010). In addition, FCD can describe functional network circuits in more detail by calculating both short-range FCD and long-range FCD (Tomasi and Volkow, 2012a, b, c). Short-range FCD refers to the density of functional connections between a given voxel and its local cluster, which represents intraregional connectivity and mainly reflects functional segregation attributes. In contrast, long-range FCD refers to the density of functional connections between the given voxel and remote voxels, which represents interregional connectivity and mainly reflects functional integration attributes (Tomasi and Volkow, 2010, 2012b). In this study, FCD analyses were focused on regions previously implicated in self- and ToM-processing.

We then conducted seed-based resting-state functional connectivity (RSFC) analyses to further investigate precise alterations in RSFC between these abnormal FCD regions and other regions at the whole-brain level. Finally, discriminant analyses were conducted to detect the patterns of RSFC that most significantly contributed to SAD diagnosis. We hypothesised that regions involved in self- and ToM-processing would exhibit altered FCD in patients with SAD, and that some patterns of RSFC associated with these regions would enable accurate diagnosis of SAD at the individual level.

Materials and methods

Participants

Twenty-three patients with SAD (six women; mean age: 21.78 ± 3.872 years) and 20 HCs (six women; mean age: 21.65 ± 3.602 years) participated in this study. Patients were recruited from the Mental Health Center of Huaxi Hospital at Sichuan University in Chengdu, China. HCs were recruited from local communities. Diagnoses of SAD were established by consensus between two attending psychiatrists and a trained interviewer using the Structured Clinical Interview DSM-IV (SCID)-Patients Version. HCs were similarly evaluated using the SCID-Patient Version to confirm the absence of psychiatric or neurological illness. All HCs were confirmed to have no history of neurological or psychiatric disorders, and no history of any major neurological or psychiatric disorders among their first-degree relatives. Inclusion criteria were as follows: (1) age between 18 and 40 years; (2) no current or past history of any neurological, psychiatric or other mental disorders except SAD; (3) absence of pregnancy, drug or alcohol abuse, organic brain disorders, or any physical illness such as hepatitis, brain tumour or epilepsy according to medical records; (4) absence of gross abnormalities on brain MRI scans (i.e. T1-weighted and T2-weighted images).

None of the participants in either group were taking psychiatric medications. All participants were evaluated using the Liebowitz Social Anxiety Scale (LSAS), Hamilton Anxiety Rating Scale (HAMA), Hamilton Depression Rating Scale (HAMD) and Spielberger State-Trait Anxiety Inventory (STAI). The STAI questionnaire consists of two components: the STAI-Trait (STAI-T) score, which represents the inherent trait anxiety of the participant, and the STAI-State (STAI-S) score, which represents the level of state anxiety at the time of test completion. STAI data were obtained prior to and following the MRI scanning session (Campbell *et al.*, 2007). Written informed consent was obtained from all participants following a thorough explanation of the procedures. This study was approved by the local Ethics Committee of Huaxi Hospital at Sichuan University and conducted in accordance with the Declaration of Helsinki (BMJ 1991; 320: 1194).

Acquisition of fMRI data

Images were acquired using a 3T GE-Signa MRI scanner (Excite, General Electric, Milwaukee, WI, USA). Thirty transverse slices (field of view [FOV] = 24 cm, in-plane matrix = 64×64, slice thickness = 5 mm, no slice gap, voxel size = $3.75 \times 3.75 \times 5$), aligned along the anterior commissure–posterior commissure (AC–PC)

line, were acquired using an echo planar imaging (EPI) sequence (time repetition [TR] = 2000 ms, time echo [TE] = 30 ms, flip angle = 90°), resulting in a total of 205 volumes for each participant. During resting fMRI scanning, participants were instructed to close their eyes, to remain as motionless as possible, not to think about anything in particular and not to fall asleep (Greicius *et al.*, 2003; Damoiseaux *et al.*, 2006; Takeuchi *et al.*, 2012). Subsequently, high-resolution T1-weighted anatomical images (TR = 8.5 ms, TE = 3.4 ms, flip angle = 12°, matrix size = 512 × 512 × 156 and voxel size = 0.47 × 0.47 × 1 mm^3) were acquired in axial orientation for each participant using a 3D spoiled gradient-recalled (SPGR) sequence.

Data pre-processing

Data processing was performed using Data Processing Assistant for Resting-State fMRI (DPARSF) software package (DPARSF, http://resting-fmri.sourceforge.net/) (Yan and Zang, 2010), implemented in Matlab (Mathworks Inc., Natick, MA, USA). Slice timing was first conducted relative to middle axial slice to correct for differences in image acquisition time between slices (Ashburner *et al.*, 2012) and realigned to correct for head motion. To reduce the impact of head motion on RSFC (Power *et al.*, 2012; Satterthwaite *et al.*, 2012; Van Dijk *et al.*, 2012), only data from participants with head movement <2.0 mm of translation and 2.0° of rotation in each axis were included. To further ensure the comparability of head movement across groups, "mean motion" was computed for each participant and compared between the groups (Van Dijk *et al.*, 2012). The images were then spatially normalised based on the Montreal Neurological Institute (MNI) EPI template provided by SPM8 and simultaneously resampled to 3 × 3 × 3 mm^3 resolution. The images were not smoothed to prevent the introduction of artificial local spatial correlations (Achard *et al.*, 2006). Finally, the data were linearly detrended and temporally band-pass filtered (0.01–0.08 Hz) to minimise the effects of low-frequency drift and high-frequency physiological noise (Cordes *et al.*, 2001). The covariates of no interest, including white matter signal, cerebrospinal fluid signal and six rigid-body head motion parameters were regressed out (Fox *et al.*, 2005). The residuals of these regressions were used for FCD analysis.

FCD analysis

FCD analyses were conducted to compute the local (lFCD) and global FCD (gFCD) at the voxel level (Tomasi and Volkow, 2010). We limited the procedure to the area within a mask created based on the Automated Anatomical Labeling (AAL) atlas (Tzourio-Mazoyer *et al.*, 2002).

Local FCD. To compute the lFCD at a given voxel *i*, the Pearson linear correlation coefficients (*R*) were first calculated to evaluate the strength of functional connectivity between time series at voxel *i* and voxels within its local cluster. Functional connections with $R > 0.44$ (corresponding to $P < 0.05$, family-wise error (FWE)-corrected) were considered significant. The lFCD at this given voxel *i* (k_i) was defined as the number of significant functional connections of voxel *i* with its local cluster.

Local clusters of voxel *i* consisted of adjacent voxels that exhibited significant functional connections with voxel *i*. A voxel *j* was added to the local cluster if it was adjacent to a voxel within the current local cluster and exhibited significant functional connectivity with voxel *i*. This algorithm was repeated for all voxels within the brain mask until no further voxels could be added to the cluster. Ultimately, the local cluster of any voxel *i* included those voxels spatially clustered and adjacent to voxel *i* whose functional connectivity with voxel *i* exceeded the given threshold.

Global FCD. The gFCD was regarded as the total number of significant functional connections between a given voxel *i* and all other voxels within the brain mask. Pearson linear correlation was used to compute functional connectivity between a voxel *i* and other voxels. A threshold of $R > 0.44$ (FWE < 0.05) was used to determine whether two voxels exhibited significant functional connectivity.

Short-range FCD and long-range FCD. In this study, we employed short- and long-range FCD for further statistical analysis (Tomasi and Volkow, 2012a, b, c). Short-range FCD is equivalent to lFCD, which detects local functional connectivity, while long-range FCD is equivalent to gFCD – lFCD, which removes connected voxels belonging to the local cluster. Short-range FCD was considered to represent intraregional connectivity; while long-range FCD was considered to represent interregional connectivity (Tomasi and Volkow, 2010, 2012b).

Finally, an isotropic Gaussian kernel (FWHM = 8 mm) was applied to long- and short-range FCD maps in SPM8 to minimise differences in the functional anatomy of the brain across participants (Tomasi and Volkow, 2010; Penny *et al.*, 2011). Furthermore, to reduce individual overall differences, long- and short-range FCD distributions were separately normalised to the average strength in the whole brain for each participant.

One-sample *t*-tests were applied with age, gender and mean head motion parameters as covariates to determine the average distributions of long- and short-range FCD in the SAD group, HC group, and in participants of both groups, respectively. Two-sample *t*-tests were conducted with the same covariates to assess group differences, independently, for long- and short-range FCD maps.

Since we aimed to investigate impairments in networks associated with self- and ToM processing in patients with SAD, group differences in FCD were assessed within regions of interest (ROIs) composed of regions that have previously been implicated in self- and ToM-processing, thresholded at FWE < 0.05, with small-volume correction (SVC) for multiple comparisons, in contiguous clusters of at least 20 voxels ($K > 20$). These regions included the bilateral ventral, dorsal and posterior cortical midline structures (CMS) (Northoff *et al.*, 2006); superior, middle and inferior temporal gyrus; TPO; and temporoparietal cortex (Han *et al.*, 2013; Schurz *et al.*, 2014). All ROIs were constructed by combining the corresponding areas in the AAL atlas (Yamada *et al.*, 2013). The ventral CMS was composed of the ACC and medial frontal cortices, while the dorsal CMS was composed of the middle cingulate cortex (MCC) and supplementary motor area, and the posterior CMS was composed of the precuneus and posterior cingulate cortex. The TPO was composed of the superior and middle TPO, and the temporoparietal cortex was composed of the angular and supramarginal gyrus.

Clusters exhibiting significant group differences were functionally defined to be ROIs, which were composed of all voxels exceeding the threshold. For the SAD group, Pearson correlation analyses were applied to test the relationship between FCD values in each ROI and LSAS fear factor, avoidance factor, and total scores, respectively. The results were thresholded at $P < 0.05$, Bonferroni corrected for multiple comparisons.

RSFC analysis

RSFC analyses were further conducted with abnormal FCD regions as seeds, in which RSFC maps for each participant were created by computing Pearson correlation coefficients between the time-varying average signals in each seed and those at remaining voxels in the grey matter mask. These correlation coefficient maps were converted into z maps using Fisher transformation to normalise the distribution, and further spatially smoothed (FWHM = 8 mm) in the same manner as the FCD maps.

The same two-sample *t*-tests used for FCD analyses were applied to assess group differences in RSFC maps. For each seed, the results were independently thresholded at $P < 0.05$, false discovery rate (FDR)-corrected for multiple comparisons at the whole-brain level ($K > 20$). Since some significant clusters covered multiple regions, functional ROIs were defined from these significant clusters by masking the AAL template (Tzourio-Mazoyer *et al.*, 2002). This process generated 14 functional ROIs, which represented regions with altered RSFC to abnormal FCD regions in patients with SAD.

Following the seed-based RSFC analysis, RSFC among all ROIs exhibiting altered RSFC to abnormal FCD regions in SAD was further examined via ROI-based functional connectivity analysis. This procedure was performed separately for ROIs that exhibited altered RSFC with abnormal short- and long-range FCD regions. The $N \times N$ (where N represents the number of ROIs) correlation matrix was computed for each participant using Pearson correlation analysis and further Fisher-z-transformed to improve the normality of the data. A two-sample *t*-test was applied on the correlation matrices to test against the hypothesis that the difference in functional connectivity between HC and patients with SAD is equal to 0. The Bonferroni method was used to correct for multiple comparisons, $P < 0.05$.

Discriminant analysis

We conducted discriminant analyses to determine which of the 14 patterns of RSFC related to abnormal FCD regions contributed most significantly to SAD diagnosis. We first created 14 functional ROIs based on clusters with significant group differences in RSFC exceeding the threshold (Nose *et al.*, 2009; Cui *et al.*, 2014). The average RSFC values of each ROI were extracted for each participant. The group was defined as the dependent variable, and the RSFC values of the 14 ROIs were defined as the independent variables for discriminant analyses. The stepwise method (significant level of enter = 0.05 and stay = 0.10) was applied to select the ROIs providing the greatest contribution to individual diagnoses. The leave-one-out method was used for classification, in which one participant was left out of the group analyses for training classifier. The leave-one-out method was further applied to redefine the ROIs based on the remaining participants' datasets, and the RSFC values corresponding to these redefined ROIs were extracted and used for the classification of this participant. When a given participant *x* was diagnosed, this participant was excluded, resulting in a total of $N-1$ participants for subsequent analyses. First, the FCD maps (including long- and short-range FCD) of the $N-1$ participants were included to assess group differences in FCD between patients with SAD and HCs, generating significant clusters that were defined as seeds, which were used to compute the seed-based RSFC map for participant *x*. Likewise, in the second step, the group difference in RSFC between the SAD and HC groups was also assessed using $N-1$ participants, and the significant clusters were redefined as ROIs that were used to extract the RSFC values of participant *x*.

Table 1. Demographic and clinical characteristics of patients with SAD and HCs

	SAD ($n = 21$)	HC ($n = 20$)	SAD *vs* HC	
	Mean ± SD	Mean ± SD	*T*	*P*
Gender	15M/6F	14M/6F	–	0.595[a]
Age (years)	22.05 ± 3.943	21.65 ± 3.602	0.337	0.738
Education (years)	14.05 ± 1.465	14.05 ± 1.959	0.004	0.996
Duration (months)	43.81 ± 39.452	–	–	–
LSAS				
Total score	53.9 ± 11.211	20.00 ± 8.265	10.976	<0.000
Fear factor	27.95 ± 6.021	8.40 ± 4.806	11.456	<0.000
Avoidance factor	25.95 ± 6.756	11.60 ± 5.906	7.227	<0.000
HAMD	7.9 ± 6.387	1.3 ± 1.867	4.540	<0.000
HAMA	6.14 ± 4.629	1.10 ± 1.744	4.657	<0.000
STAI				
STAI-T	48.14 ± 6.858	32.90 ± 4.930	8.136	<0.000
STAI-S				
Pre-scanning	41.62 ± 8.188	31.40 ± 4.849	4.831	<0.000
Post-scanning	38.29 ± 9.748	33.10 ± 7.078	1.956	0.058
Head motion	0.049 ± 0.014	0.057 ± 0.027	1.278	0.209

SD, standard deviation; SAD, social anxiety disorder; HC, healthy controls; LSAS, Liebowitz Social Anxiety Scale; HAMA, Hamilton Anxiety Rating Scale; HAMD, Hamilton Depression Rating Scale; STAI, State-Trait Anxiety Inventory.
[a]The *P* value was obtained via a chi-square test. The other *P* values were obtained via two-sample *t*-tests (two-tailed).

In addition, for those ROIs contributing to individual diagnoses, Pearson linear correlation analyses were applied in the SAD group to determine the association between the RSFC values of these ROIs and LSAS scores (fear factor, avoidance factor and total scores, respectively). The results were thresholded at $P < 0.05$, corrected for multiple comparisons using the Bonferroni method, in which $P < 0.05/n$ (where n represents the number of tests) was considered significant. In this case, n is equal to 4, the number of contributing RSFC patterns determined by the discriminant analysis.

Results

Demographic variables and clinical measures

Two patients with SAD were excluded due to excessive head motion. The demographic and clinical characteristics of the remaining 41 participants are presented in Table 1. Two sample *t*-tests were conducted to examine group differences in age, years of education, head movement and clinical characteristics. The difference in gender between the two groups was assessed via a chi-square test. Our findings revealed no significant differences in gender, age, years of education or head motion between the groups. In contrast, the SAD group exhibited significantly higher scores on the LSAS (including total, fear factor and avoidance factor scores), HAMD, HAMA, STAI-T and pre-scanning STAI-S, relative to the HC group.

FCD data

The average distributions of long- and short-range FCD in the SAD and HC groups, as well as regions in which differences in FCD were observed between the two groups, are presented in Table 2 and Figure 1.

For both the SAD and HC groups, maximal long-range FCD was observed mainly in the bilateral frontal and temporal

Table 2. Brain regions exhibiting significant differences in long- and short-range FCD between the SAD and HC groups

	Region	side	BA	t	Size	MNI		
						x	y	z
Long-range FCD								
SAD > HC	None							
SAD < HC	rACC	R	32	4.19	35	9	39	6
Short-range FCD								
SAD > HC	None							
SAD < HC	STG	R	22	4.25	63	63	−6	9

Coordinates refer to the local peak within each cluster. Results were thresholded at FWE < 0.05, SVC for multiple comparisons. rACC, rostral anterior cingulate cortex; STG, superior temporal gyrus; BA, Broadmann area; MNI, Montreal Neurological Institute; L, left hemisphere; R, right hemisphere; SAD, social anxiety disorder; HC, healthy control.

cortices, temporal parietal junction areas, anterior and posterior medial regions, subcortical and occipital cortices. In contrast, maximal short-range FCD was mainly observed in the bilateral occipital, posteromedial and frontal cortices. Regions with high FCD are regarded as functional hubs of brain networks, which are thought to play critical roles in the brain. The FCD hubs observed in this study are consistent with those identified in previous studies (Buckner *et al.*, 2009; Tomasi and Volkow, 2011; Ding *et al.*, 2013). Two sample *t*-tests within ROIs revealed significantly lower long-range FCD in patients with SAD relative to HCs in the right rACC (BA 32, local maximum at $x = 9$, $y = 39$, $z = 6$, $P = 0.027$ corrected for FWE at the voxel level within the right ventral CMS region). Similarly, significantly lower short-range FCD was observed in the right STG (BA 22, local maximum at $x = 63$, $y = -6$, $z = 9$, $P = 0.013$ corrected for FWE at the voxel level within the right STG region) of the SAD group. No significant correlation was observed between any LSAS scores and FCD values in either long- or-short range abnormal FCD regions.

RSFC data

The results of seed-based RSFC analysis of regions exhibiting altered RSFC with abnormal long- and short-range FCD regions are presented in Table 3 and Figure 2.

In the SAD group, significantly decreased RSFC was observed between the rACC seed (the abnormal long-range FCD region) and other widely distributed brain regions, including the left and right superior frontal gyrus (SFG), right middle frontal gyrus (MFG), right STG and posteromedial regions spanning the left and right MCC and precuneus.

Significantly decreased RSFC of the right STG seed (the abnormal short-range FCD region) was also observed in patients with SAD. Such alterations were observed in the right inferior frontal gyrus (IFG), left supplementary motor area (SMA), bilateral precentral gyrus (PRCG), postcentral gyrus (PTCG) and right putamen, left and right STG, right middle TPO, and right insula.

The results of ROI-based RSFC analysis of RSFC among regions exhibiting altered RSFC with abnormal long- and short-range FCD regions are illustrated in Figure 3. Our results indicated that RSFC among regions exhibiting altered RSFC with the right rACC did not significantly differ between the SAD and HC groups. In contrast, significant differences in RSFC among regions exhibiting altered RSFC with the right STG were observed between the groups: Patients with SAD exhibited decreased RSFC between the right STG and right PRCG, PTCG and right insula; between the right PRCG and right insula, right putamen, and right PTCG; and between the right putamen and right PTCG.

Discriminant analysis

The results of the discriminant analyses are shown in Figure 4. Among the 14 patterns of altered RSFC associated with abnormal FCD regions, 4 such patterns provided the greatest contribution to individual diagnosis: 3 corresponding to the right rACC ([right rACC–right SFG], [right rACC–left SFG] and [right rACC–right MFG]) and 1 corresponding to the right STG ([right STG–right STG]) (canonical coefficient = 0.752, eigenvalue = 1.298, Wilks' Lambda = 0.435, $P < 0.001$). Cross-validation classification achieved a sensitivity of 90.5%, specificity of 80% and an accuracy of 85.4%. No significant correlation was observed between any of the LSAS scores and values of the four contributing RSFC patterns.

Discussion

This study marks the first application of FCD analysis in conjunction with RSFC and discriminant analyses for the detection of impairments in networks associated with self- and ToM-processing in patients with SAD. FCD analysis provided general information regarding whether a region exhibited altered connection density with other regions at the whole-brain level, while RSFC provided more precise information regarding specific connectivity involving abnormal FCD regions. Finally, discriminant analysis allowed us to determine which patterns of alteration could be used to diagnose SAD at the individual level. Combined use of these three methods enabled us to explore potential impairments in self- and ToM-related networks in a systematic fashion by gradually investigating the general, specific and critical characteristics of impaired networks in SAD.

Patients with SAD exhibited decreased long-range FCD in the right rACC, a key node associated with self-processing (Northoff *et al.*, 2006; Moeller and Goldstein, 2014), as well as decreased short-range FCD in the right STG, a key node associated with social cognition (Lahnakoski *et al.*, 2012; Beauchamp, 2015). Regions exhibiting decreased RSFC with the right rACC included the frontal, temporal and posteromedial regions, though no differences in RSFC among these regions were observed between the two groups. In contrast, regions exhibiting decreased RSFC with the right STG included the temporal, sensorimotor, somatosensory and frontal regions, and RSFC among these regions was attenuated in patients with SAD. Furthermore, discriminant analysis indicated that, among the altered patterns of RSFC involving two abnormal regions, [right rACC–bilateral SFG], [right rACC–right MFG] and [right STG–right STG] connectivity contributed most substantially to distinction between participants of the SAD and HC groups, with an accuracy of 85.4%. These results aligned with our hypothesis that SAD involves impairments in networks associated with self- and ToM-processing, providing new insight into our understanding of the neural pathomechanism of SAD.

Impairments associated with self-processing

Patients of the SAD group exhibited decreased long-range FCD in the right rACC. Given that the rACC exhibits strong connections with frontal and limbic systems, it has been implicated in emotional processing and emotional conflict (Etkin *et al.*, 2011). In addition, the rACC is considered a key node of the self-referential network (SRN) (Northoff *et al.*, 2006), and many recent studies

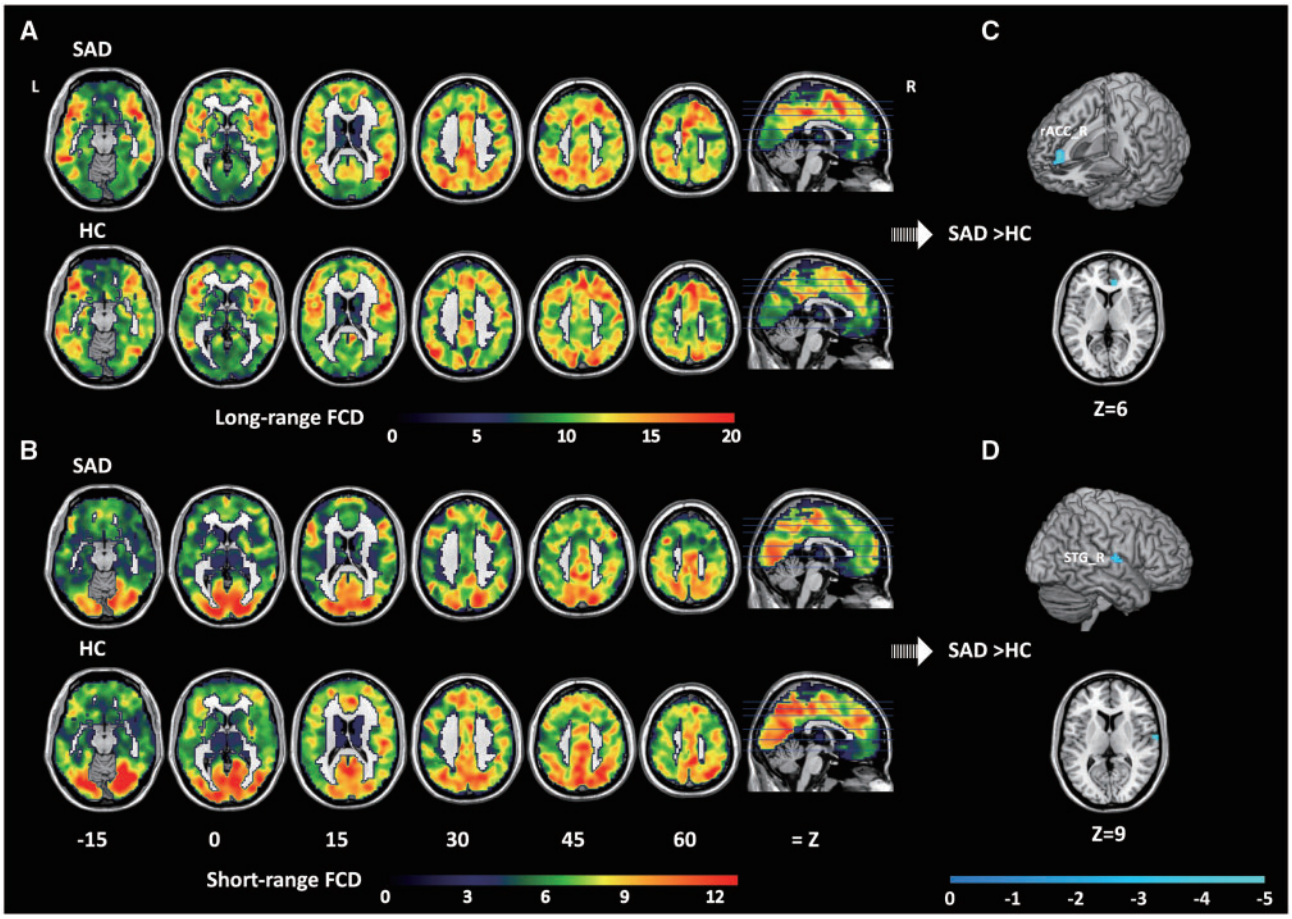

Fig. 1. Results of FCD analysis. Distribution of long-range (A) and short-range (B) FCD in the brain for the SAD and HC groups. Brain regions exhibiting significant differences in long-range (C) and short-range (D) FCD between the two groups. For (C) and (D), significant clusters are shown on the surface-rendered brain, and in axial (Z) views at the peak effect coordinates. All maps are thresholded at FWE < 0.05, with SVC for multiple comparisons, in a contiguous cluster of at least 20 voxels ($K > 20$). Colour bars represent t values. rACC, rostral anterior cingulate cortex; STG, superior temporal gyrus; L, left hemisphere; R, right hemisphere; FCD, functional connectivity density; SAD, social anxiety disorder; HC, healthy control.

have confirmed the affective role of the rACC in self-referential processing (van der Meer *et al.*, 2010), emotional tagging of stimuli with personal relevance (Moeller and Goldstein, 2014) and self-referential processing of negative stimuli (Yoshimura *et al.*, 2009). Decreased long-range FCD in the rACC may be indicative of impairments in networks associated with emotional self-referential processing in patients with SAD, which may manifest as decreased interregional connectivity between the rACC and regions involved in various functional networks.

RSFC analysis further revealed that the prefrontal cortices (PFC), STG and posteromedial regions exhibited decreased RSFC with the rACC, while the RSFCs among these regions themselves exhibited no alterations in patients with SAD. This finding is consistent with the assumption of long-range FCD, which represents the interregional connection between a given voxel and remote voxels that likely belong to different networks than voxel *i* (Tomasi and Volkow, 2010, 2012b).

Previous studies have repeatedly revealed the PFC to be involved in cognitive control (Tully *et al.*, 2014; De Baene *et al.*, 2015). The posteromedial region of the PFC is considered a hub of the SRN (Parvizi *et al.*, 2006), which likely plays a role in integrating information from multiple domains during self-processing (Cavanna and Trimble, 2006). And the STG has been implicated in ToM-processing (Schurz *et al.*, 2014). The widely attenuated connections between the rACC and these regions observed in this study may be indicative of widespread attenuated cooperation among emotional self-referential processing, cognitive control, ToM and the integration of self-related information.

Among these widely attenuated connections, the rACC and PFC regions provided the greatest contribution to individual diagnoses of SAD. This finding is consistent with the previous behavioural observation that patients with SAD exhibit impairments in cognitive control (Werner *et al.*, 2011; D'Avanzato *et al.*, 2013), and with those of previous neuroimaging studies. Such imaging studies have reported that patients with SAD exhibit reduced and temporally delayed PFC activation during down-regulating negative emotional reactivity to negative evaluation of self- and social threat stimuli (Goldin *et al.*, 2009a, b) and decreased functional connectivity between the PFC and various regions at rest (Liao *et al.*, 2010). Considering the role that the rACC plays in emotional self-referential processing, especially for negative stimuli (Yoshimura *et al.*, 2009), the decreased functional connectivity between PFC and rACC may reflect a lack of cognitive inhibition on such processes, leading to an impaired ability to disengage from negative self-reflection (Matthews *et al.*, 2009). This mechanism may be a foundation for the distorted negative self-beliefs observed in SAD (Morrison and Heimberg, 2013). Negative self-

Table 3. Brain regions exhibiting significant differences in RSFC with the abnormal FCD regions (in italic) between the SAD and HC groups

	Regions	Side	BA	t	Size	MNI		
						x	y	z
Right rACC								
SAD >HC	None							
SAD <HC								
Cluster 1	STG	R	21	5.73	105	69	−12	−6
Cluster 2	Precuneus/MCC	R/L	7/31	5.59	426	0	−30	48
Cluster 3	SFG[a]	L	9	4.82	35	−18	45	36
Cluster 4	MFG[a]	R	6/8	4.47	58	30	15	60
Cluster 5	SFG[a]	R	10	4.21	45	15	63	18
Right STG								
SAD >HC	None							
SAD <HC								
Cluster 1	STG	L	43/41/22/42	5.34	344	−54	−12	9
Cluster 2	Insula	R	13/21/22	5.02	262	33	6	6
	Putamen	R						
Cluster 3	STG[a]	R	42/43/21/21	4.97	385	66	−18	9
Cluster 4	PTCG/PRCG	R	4/6/3	4.52	180	51	−18	54
Cluster 5	Middle TPO	R	38	4.33	26	30	15	−39
Cluster 6	PRCG/PTCG	L	4/6	4.30	97	−42	−15	54
Cluster 7	SMA	L	6/24	3.93	44	−3	−6	54
Cluster 8	IFG	R	46	3.88		57	30	27

Coordinates refer to the local peak within each cluster. Results were thresholded at FDR < 0.05, $K > 20$. rACC, rostral anterior cingulate cortex; STG, superior temporal gyrus; MCC, middle cingulate cortex; SFG, superior frontal gyrus; MFG, middle frontal gyrus; PTCG, postcentral gyrus; PRCG, precentral gyrus; TPO, temporal pole; SMA, supplementary area; IFG, inferior frontal gyrus. BA, Broadmann area; MNI, Montreal Neurological Institute; L, left hemisphere; R, right hemisphere; SAD, social anxiety disorder; HC, healthy control.

[a]RSFC between these regions and the abnormal FCD regions contributed most substantially to SAD diagnosis

beliefs can exaggerate negative emotions and disturb emotional regulation, and in turn, serve to maintain anxiety (Spurr and Lusia, 2002). Indeed, previous studies have reported that patients with SAD exhibit difficulties in emotional regulation (Etkin and Wager, 2007), and that the rACC is also involved in regulating emotional conflict (Etkin *et al.*, 2011).

Impaired connectivity associated with ToM-processing

Patients with SAD exhibited decreased short-range FCD in the right STG, a nexus of social cognition (Lahnakoski *et al.*, 2012; Beauchamp, 2015) and is substantially involved in ToM-processing (Schurz *et al.*, 2014). Decreased short-range FCD in the STG may therefore indicate impairments in networks associated with ToM-processing, which may in turn manifest as decreased intraregional connections between the STG and its local cluster (Tomasi and Volkow, 2010, 2012b).

RSFC analysis further revealed that the temporal, sensorimotor, somatosensory and frontal regions exhibited decreased RSFC with the STG in patients with SAD, and that the RSFC among these regions themselves also exhibited significant decreases. This finding is consistent with the assumption of short-range FCD, which represents the intraregional connectivity between a given region and its local cluster (Tomasi and Volkow, 2010, 2012b). Therefore, regions belonging to the local cluster of the STG are likely involved in STG-relevant functions.

Our findings further support this hypothesis, as the regions exhibiting altered RSFC with the STG are primarily involved in ToM and ToM-relevant social processing. The temporal regions exhibiting altered connectivity with the STG included the bilateral STG and right middle TPO. The TPO is a key node of ToM-processing (Olson et al., 2007; Takahashi et al., 2008; Yamada et al., 2012), playing an important role in accessing social knowledge while reasoning regarding the mental states of others (Frith and Frith, 2005; Pantazatos *et al.*, 2014). Furthermore, sensorimotor regions including the bilateral PRCG, left SMA and right putamen have been implicated in social perception, playing a role in the detection of others' intentions via observation of biological motion cues (Adolphs, 2001). The somatosensory region including the insula is involved in the processing of socially relevant emotional information (Lamm and Singer, 2010) and social perception, with previous research suggesting that this region performs a type of emotional simulation in order to determine the feelings and intentions of others (Keysers *et al.*, 2010; Schurz *et al.*, 2014). The broadly attenuated connections between these ToM-related regions and the STG may therefore suggest impaired communication among regions of the ToM-related network in patients with SAD.

Discriminant analysis further revealed that decreased RSFC within the right STG contributed most substantially to individual diagnoses of SAD. Considering the integrative role of the STG in ToM-processing (Lahnakoski *et al.*, 2012), difficulties in integrating social information from multiple domains may play an important role in maladaptive ToM in SAD. Such impairments may contribute to common characteristics of SAD, including biased perception of others' mental states (O'Toole *et al.*, 2013), misunderstanding of social situations (Morrison and Heimberg, 2013), and lack of social skills to generate contextually appropriate social responses (Mesa *et al.*, 2015).

Limitations

This study possesses some limitations of note. First, we used a leave-one-out analysis to examine the validity of altered

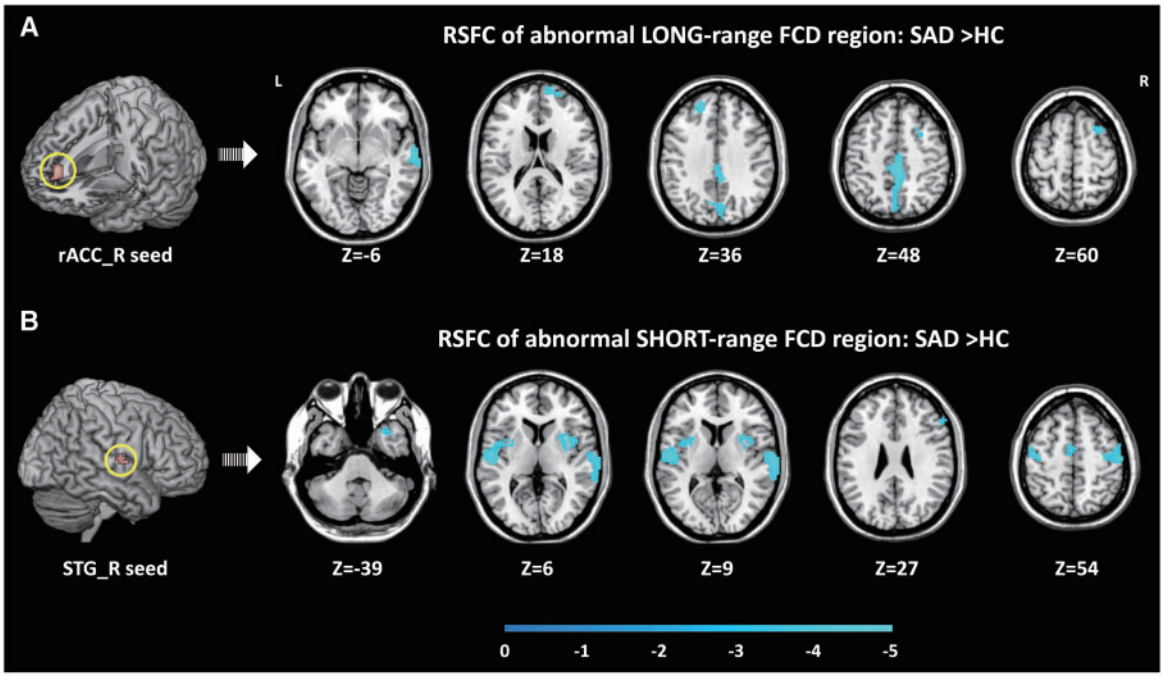

Fig. 2. Results of seed-based RSFC analysis. Brain regions exhibiting altered RSFC with the abnormal long-range (A) and short-range (B) FCD regions in patients with SAD. Within each sub-figure, significant clusters are shown in axial (*Z*) views at the peak effect coordinates. All maps are thresholded at FDR < 0.05, $K > 20$. Colour bars represent *t* values. rACC, rostral anterior cingulate cortex; STG, superior temporal gyrus; L, left hemisphere; R, right hemisphere; FCD, functional connectivity density; RSFC, resting-state functional connectivity; SAD, social anxiety disorder; HC, healthy control.

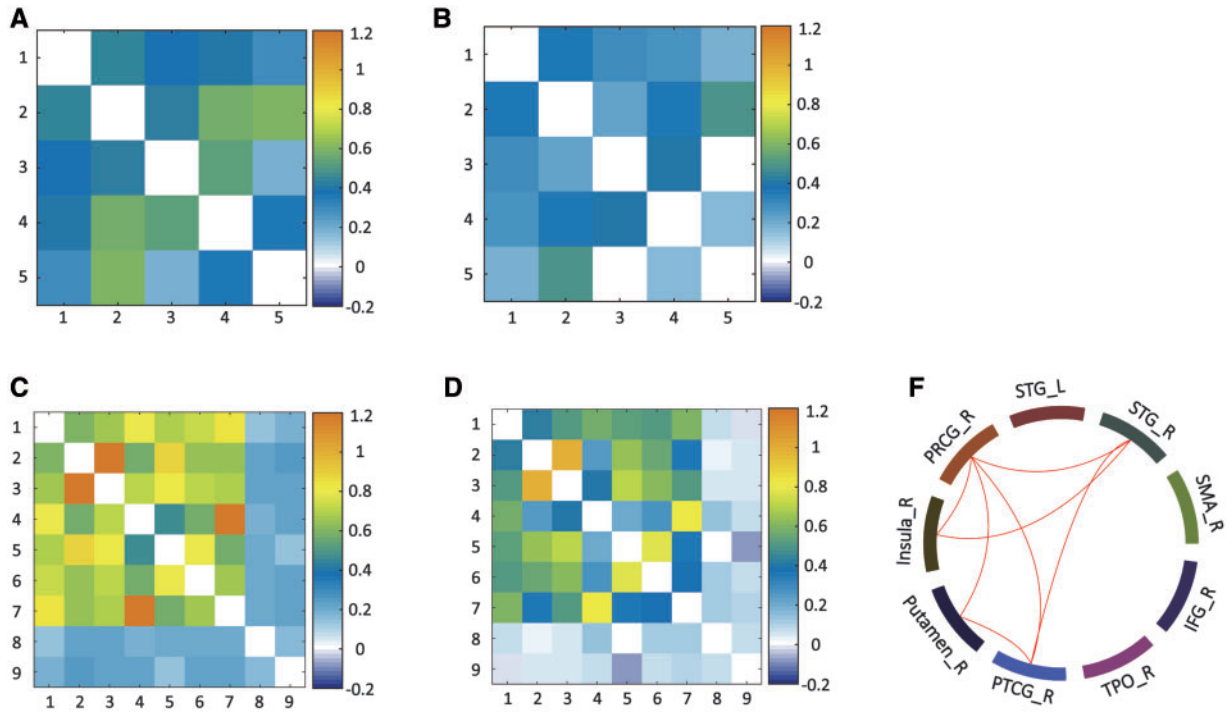

Fig. 3. Results of ROI-based RSFC analysis. The correlation matrix among ROIs exhibiting altered RSFC with the abnormal long-range FCD region (the right rACC) are shown for the HC (A) and SAD (B) groups. Similarly, the correlation matrix among ROIs exhibiting altered RSFC with the abnormal short-range FCD region (the right STG) are also shown for the HC (C) and SAD (D) groups. The colour bar indicates the Fisher-z values. RSFC among most regions exhibiting altered RSFC with the right STG was decreased in patients with SAD (red line, Bonferroni correction) (F). However, RSFC among regions exhibiting altered RSFC with the right rACC did not significantly differ between the groups. STG, superior temporal gyrus; PTCG, postcentral gyrus; PRCG, precentral gyrus; TPO, temporal pole; IFG, inferior frontal gyrus; SMA, supplementary area; L, left hemisphere; R, right hemisphere.

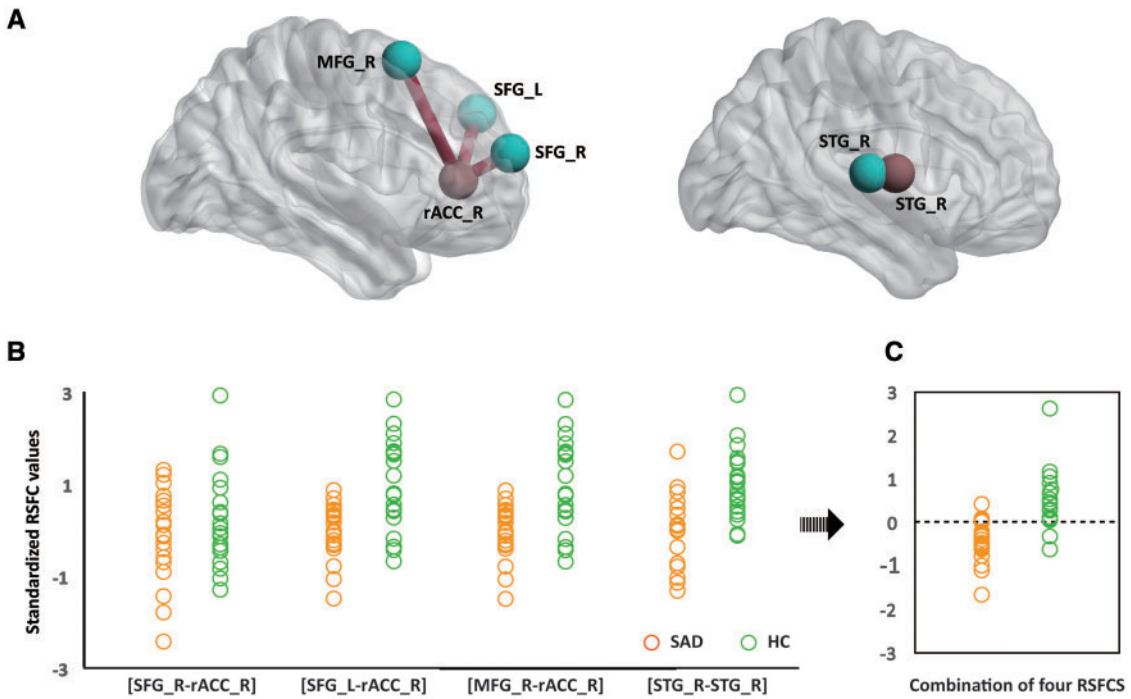

Fig. 4. Results of discriminant analysis. RSFC among four brain regions (blue) and two abnormal FCD regions (red) contributed most substantially to individual diagnoses of SAD (A). Standardised values of each contributing RSFC pattern for each participant of the SAD (orange) and HC (green) group are shown (B). The discriminant analysis based on the four contributing RSFC patterns obtained an accuracy of 85.4% (C). The dotted line represents the value of the threshold for the classification (canonical coefficient = 0.752, eigenvalue = 1.298, Wilks' Lambda = 0.435, $P < 0.001$) (D). rACC, rostral anterior cingulate cortex; STG, superior temporal gyrus; SFG, superior frontal gyrus; MFG, middle frontal gyrus; L, left hemisphere; R, right hemisphere; RSFC, resting-state functional connectivity; SAD, social anxiety disorder; HC, healthy control.

connectivity in determining individual diagnoses of SAD. However, since our sample was relatively small, and all data had the same imaging parameters, future studies utilising larger independent samples are required to confirm our findings. Second, although we controlled for the level of education in this study, we did not obtain information regarding basic cognitive abilities. Since many studies have documented strong associations among cognitive abilities, academic performance (Kuncel *et al.*, 2004) and education level (Wai, 2014), we believe our method indirectly accounted for the effect of cognitive ability. However, caution is required in future studies, especially when attempting to account for cognitive abilities that are not relevant to education level but may strongly affect brain function. Third, due to the observational nature of this study, and the ambiguous boundary between neural mechanisms involved in self- and ToM-processing (Spreng *et al.*, 2009; Denny *et al.*, 2012), the precise contributions of impaired self- and ToM-processing to SAD cannot be drawn from measures of functional connectivity alone.

Conclusion

This study provides evidence that SAD is associated with impairments in neural networks involved in self- and ToM-processing, highlighting that the pathomechanism of SAD may be associated with alterations in the recognition of internal and social worlds. However, future neuroimaging studies based on specific tasks are required to elucidate the precise associations between impaired self- and ToM-processing and brain features in SAD.

Funding

This study was supported by the 863 Project [2015AA020505]; The Natural Science Foundation of China [61533006, 31400901, 31600930 and 61673089]; the Science Foundation of Ministry of Education of China [14XJC190003]; and the Fundamental Research Funds for the Central Universities of China [ZYGX2013Z004 and ZYGX2014J104].

Conflict of interest. None declared.

References

Achard, S., Salvador, R., Whitcher, B., Suckling, J., Bullmore, E.D. (2006). A resilient, low-frequency, small-world human brain functional network with highly connected association cortical hubs. *The Journal of Neuroscience*, **26**, 63–72.

Adolphs, R. (2001). The neurobiology of social cognition. *Current Opinion in Neurobiology*, **11**, 231–9.

Ashburner, J., Gareth, B., Chun-Chuan, C., *et al.* (2012) *SPM8 Manual*. Functional Imaging Laboratory, Institute of Neurology.

American Psychiatric Association. (2013) Diagnostic and statistical manual of mental disorders (DSM-5®): American Psychiatric Association.

Beauchamp, M.S. (2015). The social mysteries of the superior temporal sulcus. *Trends in Cognitive Sciences*, **19**, 489–90.

Buckner, R.L., Sepulcre, J., Talukdar, T., *et al.* (2009). Cortical hubs revealed by intrinsic functional connectivity: mapping, assessment of stability, and relation to Alzheimer's disease. *Journal of Neuroscience*, **29**, 1860–73.

Buhlmann, U., Wacker, R., Dziobek, I. (2015). Inferring other people's states of mind: comparison across social anxiety, body dysmorphic, and obsessive-compulsive disorders. *Journal of Anxiety Disorders*, **34**, 107–13.

Campbell, D. W., Sareen, J., Paulus, M. P., Goldin, P. R., Stein, M. B., Reiss, J. P. (2007). Time-varying amygdala response to emotional faces in generalized social phobia. *Biological Psychiatry*, **62**, 455–63.

Cavanna, A.E., Trimble, M.R. (2006). The precuneus: a review of its functional anatomy and behavioural correlates. *Brain*, **129**, 564–83.

Cordes, D., Haughton, V. M., Arfanakis, K., *et al.* (2001). Frequencies contributing to functional connectivity in the cerebral cortex in "resting-state" data. *American Journal of Neuroradiology*, **22**, 1326–33.

Cui, Q., Vanman, E. J., Wei, D., Yang, W., Jia, L., Zhang, Q. (2014). Detection of deception based on fMRI activation patterns underlying the production of a deceptive response and receiving feedback about the success of the deception after a mock murder crime. *Social Cognitive and Affective Neuroscience*, **9**, 1472–80.

D'Avanzato, C., Joormann, J., Siemer, M., Gotlib, I.H. (2013). Emotion regulation in depression and anxiety: examining diagnostic specificity and stability of strategy use. *Cognitive Therapy and Research*, **37**, 968–80.

Damoiseaux, J. S., Rombouts, S. A. R. B., Barkhof, F., *et al.* (2006). Consistent resting-state networks across healthy subjects. *Proceedings of the National Academy of Sciences of the United States of America*, **103**, 13848–53.

De Baene, W., Duyck, W., Brass, M., Carreiras, M. (2015). Brain circuit for cognitive control is shared by task and language switching. *Journal of Cognitive Neuroscience*, **27**, 14–1.

Declaration of Helsinki (BMJ 1991; 302: 1194).

Denny, B.T., Kober, H., Wager, T.D., Ochsner, K.N. (2012). A meta-analysis of functional neuroimaging studies of self- and other judgments reveals a spatial gradient for mentalizing in medial prefrontal cortex. *Journal of Cognitive Neuroscience*, **24**, 1742–52.

Ding, J., An, D., Liao, W., *et al.* (2013). Altered functional and structural connectivity networks in psychogenic non-epileptic seizures. *PLoS One* **8**, e63850.

Etkin, A., Egner, T., Kalisch, R. (2011). Emotional processing in anterior cingulate and medial prefrontal cortex. *Trends in Cognitive Sciences*, **15**, 85–93.

Etkin, A., Wager, T.D. (2007). Functional neuroimaging of anxiety: a meta-analysis of emotional processing in PTSD, social anxiety disorder, and specific phobia. *American Journal of Psychiatry*, **164**, 1476–88.

Fox, M. D., Snyder, A. Z., Vincent, J. L., Corbetta, M., Van Essen, D. C., Raichle, M. E. (2005). The human brain is intrinsically organized into dynamic, anticorrelated functional networks. *Proceedings of the National Academy of Sciences of the United States of America*, **102**, 9673–8.

Frith, C., Frith, U. (2005). Theory of mind. *Current Biology*, **15**, R644–5.

Goldin, P., Ziv, M., Jazaieri, H., Gross, J.J. (2012). Randomized controlled trial of mindfulness-based stress reduction versus aerobic exercise: effects on the self-referential brain network in social anxiety disorder. *Frontiers in Human Neuroscience*, **6**, 295.

Goldin, P. R., Ziv, M., Jazaieri, H., Hahn, K., Gross, J.J. (2013a). MBSR vs aerobic exercise in social anxiety: fMRI of emotion regulation of negative self-beliefs. *Social Cognitive and Affective Neuroscience*, **8**, 65–72.

Goldin, P. R., Ziv, M., Jazaieri, H., Hahn, K., Heimberg, R., Gross, J. J. (2013b). Impact of cognitive behavioral therapy for social anxiety disorder on the neural dynamics of cognitive reappraisal of negative self-beliefs: randomized clinical trial. *JAMA Psychiatry*, **70**, 1048–56.

Goldin, P.R., Manber-Ball, T., Werner, K., Heimberg, R., Gross, J.J. (2009a). Neural mechanisms of cognitive reappraisal of negative self-beliefs in social anxiety disorder. *Biological Psychiatry*, **66**, 1091–9.

Goldin, P.R., Manber, T., Hakimi, S., Gross, J.J. (2009b). Neural bases of social anxiety disorder: emotional reactivity and cognitive regulation during social and physical threat. *Archives of General Psychiatry*, **66**, 170–80.

Goldin, P. R., Ziv, M., Jazaieri, H., Weeks, J., Heimberg, R. G., Gross, J. J. (2014). Impact of cognitive-behavioral therapy for social anxiety disorder on the neural bases of emotional reactivity to and regulation of social evaluation. *Behaviour Research and Therapy*, **62**, 97–106.

Greicius, M.D., Krasnow, B., Reiss, A.L., Menon, V. (2003). Functional connectivity in the resting brain: a network analysis of the default mode hypothesis. *Proceedings of the National Academy of Sciences of the United States of America*, **100**, 253–8.

Han, S., Northoff, G., Vogeley, K., Wexler, B. E., Kitayama, S., Varnum, M. E. (2013). A cultural neuroscience approach to the biosocial nature of the human brain. *Annual Review of Psychology*, **64**, 335–59.

Heitmann, C. Y., Jutta, P., Martin, M. L., *et al.* (2014). Neural correlates of anticipation and processing of performance feedback in social anxiety. *Human Brain Mapping*, **35**, 6023–31.

Hezel, D.M., McNally, R.J. (2014). Theory of mind impairments in social anxiety disorder. *Behavior Therapy*, **45**, 530–40.

Keysers, C., Kaas, J.H., Gazzola, V. (2010). Somatosensation in social perception. *Nature Reviews Neuroscience*, **11**, 417–28.

Kilts, C. D., Kelsey, J. E., Bettina, K., *et al.* (2006). The neural correlates of social anxiety disorder and response to pharmacotherapy. *Neuropsychopharmacology*, **31**, 2243–53.

Klumpp, H., Fitzgerald, D.A., Angstadt, M., Post, D., Phan, K.L. 2014). Neural response during attentional control and emotion processing predicts improvement after cognitive behavioral therapy in generalized social anxiety disorder. *Psychological Medicine*, **44**, 3109–21.

Kuncel, N.R., Hezlett, S.A., Ones, D.S. (2004). Academic performance, career potential, creativity, and job performance: can one construct predict them all? *Journal of Personality and Social Psychology*, **86**, 148.

Lahnakoski, J. M., Glerean, E., Salmi, J., *et al.* (2012). Naturalistic fMRI mapping reveals superior temporal sulcus as the hub for the distributed brain network for social perception. *Frontiers in Human Neuroscience*, **6**, 1–13.

Lamm, C., Singer, T. (2010). The role of anterior insular cortex in social emotions. *Brain Structure and Function*, **214**, 579–91.

Liao, W., Chen, H., Feng, Y., *et al.* (2010). Selective aberrant functional connectivity of resting state networks in social anxiety disorder. *NeuroImage*, **52**, 1549–58.

Liu, F., Guo, W., Fouche, J.-P., *et al.* (2013). Multivariate classification of social anxiety disorder using whole brain functional connectivity. *Brain Structure and Function*, **220**, 1–15.

Liu, F., Zhu, C., Wang, Y., *et al.* (2014). Disrupted cortical hubs in functional brain networks in social anxiety disorder. *Clinical Neurophysiology*, **126**, 1711–6.

Matthews, S., Simmons, A., Strigo, I., Gianaros, P., Yang, T., Paulus, M. (2009). Inhibition-related activity in subgenual cingulate is associated with symptom severity in major depression. *Psychiatry Research: Neuroimaging*, **172**, 1–6.

Mesa, F., Le, T.-A., Beidel, D. (2015) Social skill-based treatment for social anxiety disorder in adolescents, in Ranta, K., La Greca, A. M., Garcia-Lopez L.-J., Marttunen, M., editors. *Social Anxiety and Phobia in Adolescents*, Springer International Publishing.

Moeller, S.J., Goldstein, R.Z. (2014). Impaired self-awareness in human addiction: deficient attribution of personal relevance. *Trends in Cognitive Sciences*, **18**, 635–41.

Morrison, A.S., Heimberg, R.G. (2013). Social anxiety and social anxiety disorder. *Annual Review of Clinical Psychology*, **9**, 249–74.

Moscovitch, D.A. (2009). What is the core fear in social phobia? A new model to facilitate individualized case conceptualization and treatment. *Cognitive and Behavioral Practice* **16**, 123–34.

Northoff, G., Heinzel, A., de Greck, M., Bermpohl, F., Dobrowolny, H., Panksepp, J. (2006). Self-referential processing in our brain—a meta-analysis of imaging studies on the self. *NeuroImage*, **31**, 440–57.

Nose, I., Murai, J., Taira, M. (2009). Disclosing concealed information on the basis of cortical activations. *NeuroImage*, **44**, 1380–6.

O'Toole, M.S., Hougaard, E., Mennin, D.S. (2013). Social anxiety and emotion knowledge: a meta-analysis. *Journal of Anxiety Disorders*, **27**, 98–108.

Olson, I.R., Plotzker, A., Ezzyat, Y. (2007). The Enigmatic temporal pole: a review of findings on social and emotional processing. *Brain*, **130**, 1718–31.

Pantazatos, S.P., Talati, A., Schneier, F.R., Hirsch, J. (2014). Reduced anterior temporal and hippocampal functional connectivity during face processing discriminates individuals with social anxiety disorder from healthy controls and panic disorder, and increases following treatment. *Neuropsychopharmacology*, **39**, 425–34.

Parvizi, J., Van Hoesen, G.W., Buckwalter, J., Damasio, A. (2006). Neural connections of the posteromedial cortex in the macaque. *Proceedings of the National Academy of Sciences of the United States of America*, **103**, 1563–8.

Penny, W.D., Friston, K.J., Ashburner, J.T., Kiebel, S.J., Nichols, T.E. (2011) *Statistical Parametric Mapping: The Analysis of Functional Brain Images: The Analysis of Functional Brain Images*, London: Academic Press.

Phan, K.L., Fitzgerald, D.A., Nathan, P.J., Tancer, M.E. (2006). Association between amygdala hyperactivity to harsh faces and severity of social anxiety in generalized social phobia. *Biological Psychiatry*, **59**, 424–9.

Power, J.D., Barnes, K.A., Snyder, A.Z., Schlaggar, B.L., Petersen, S.E. (2012). Spurious but systematic correlations in functional connectivity MRI networks arise from subject motion. *NeuroImage*, **59**, 2142–54.

Satterthwaite, T. D., Wolf, D. H., Loughead, J., *et al.* (2012). Impact of in-scanner head motion on multiple measures of functional connectivity: relevance for studies of neurodevelopment in youth. *NeuroImage*, **60**, 623–32.

Schurz, M., Radua, J., Aichhorn, M., Richlan, F., Perner, J. (2014). Fractionating theory of mind: a meta-analysis of functional brain imaging studies. *Neuroscience & Biobehavioral Reviews*, **42**, 9–34.

Spreng, R.N., Mar, R.A., Kim, A.S. (2009). The common neural basis of autobiographical memory, prospection, navigation, theory of mind, and the default mode: a quantitative meta-analysis. *Journal of Cognitive Neuroscience*, **21**, 489–510.

Spurr, J.M., Lusia, S. (2002). Self-focused attention in social phobia and social anxiety. *Clinical Psychology Review*, **22**, 947–75.

Stein, M.B., Stein, D.J. (2008). Social anxiety disorder. *Lancet*, **371**, 1115–25.

Takahashi, H., Matsuura, M., Koeda, M., *et al.* (2008). Brain activations during judgments of positive self-conscious emotion and positive basic emotion: pride and joy. *Cerebral Cortex*, **18**, 898–903.

Takeuchi, H., Taki, Y., Hashizume, H., *et al.* (2012). The association between resting functional connectivity and creativity. *Cerebral Cortex*, **22**, 2921–9.

Talati, A., Pantazatos, S.P., Schneier, F.R., Weissman, M.M., Hirsch, J. (2013). Gray matter abnormalities in social anxiety disorder: primary, replication, and specificity studies. *Biological Psychiatry*, **73**, 75–84.

Tillfors, M., Furmark, T., Marteinsdottir, I., Fredrikson, M. (2002). Cerebral blood flow during anticipation of public speaking in social phobia: a PET study. *Biological Psychiatry*, **52**, 1113–9.

Tomasi, D., Volkow, N.D. (2010). Functional connectivity density mapping. *Proceedings of the National Academy of Sciences of the United States of America*, **107**, 9885–90.

Tomasi, D., Volkow, N.D. (2011). Functional connectivity hubs in the human brain. *NeuroImage*, **57**, 908–17.

Tomasi, D., Volkow, N.D. (2012a). Abnormal functional connectivity in children with attention-deficit/hyperactivity disorder. *Biological Psychiatry*, **71**, 443–50.

Tomasi, D., Volkow, N.D. (2012b). Aging and functional brain networks. *Molecular Psychiatry*, **17**, 549–58.

Tomasi, D., Volkow, N.D. (2012c). Gender differences in brain functional connectivity density. *Human Brain Mapping*, **33**, 849–60.

Tully, L.M., Lincoln, S.H., Liyanage-Don, N., Hooker, C.I. (2014). Impaired cognitive control mediates the relationship between cortical thickness of the superior frontal gyrus and role functioning in schizophrenia. *Schizophrenia Research*, **152**, 358–64.

Tzourio-Mazoyer, N., Landeau, B., Papathanassiou, D., *et al.* (2002). Automated anatomical labeling of activations in SPM using a macroscopic anatomical parcellation of the MNI MRI single-subject brain. *NeuroImage*, **15**, 273–89.

van der Meer, L., Costafreda, S., Aleman, A., David, A.S. (2010). Self-reflection and the brain: a theoretical review and meta-analysis of neuroimaging studies with implications for schizophrenia. *Neuroscience & Biobehavioral Reviews*, **34**, 935–46.

Van Dijk, K.R., Sabuncu, M.R., Buckner, R.L. (2012). The influence of head motion on intrinsic functional connectivity MRI. *NeuroImage*, **59**, 431–8.

Wai, J. (2014). Experts are born, then made: combining prospective and retrospective longitudinal data shows that cognitive ability matters. *Intelligence*, **45**, 74–80.

Werner, K.H., Goldin, P.R., Ball, T.M., Heimberg, R.G., Gross, J.J. (2011). Assessing emotion regulation in social anxiety disorder: the emotion regulation interview. *Journal of Psychopathology and Behavioral Assessment*, **33**, 346–54.

Yamada, M., Camerer, C. F., Fujie, S., *et al.* (2012). Neural circuits in the brain that are activated when mitigating criminal sentences. *Nature Communications*, **3**, 759.

Yamada, M., Uddin, L. Q., Takahashi, H., *et al.* (2013). Superiority illusion arises from resting-state brain networks modulated by

dopamine. *Proceedings of the National Academy of Sciences of the United States of America* **110**, 4363–7.

Yan, C., Zang, Y. (2010). DPARSF: a MATLAB toolbox for "Pipeline" data analysis of resting-state fMRI. *Frontiers in Systems Neuroscience*, **4**, 13.

Yoshimura, S., Ueda, K., Suzuki, S.-i., Onoda, K., Okamoto, Y., Yamawaki, S. (2009). Self-referential processing of negative stimuli within the ventral anterior cingulate gyrus and right amygdala. *Brain and Cognition*, **69**, 218–25.